



Molecular Crystals and Liquid Crystals

Publication details, including instructions for authors and subscription information:

<http://www.tandfonline.com/loi/gmcl16>

The Structure and Conformation of n-Hydrocarbon Chains in Bilayer Systems in the "Fluid" Phase

Michele Vacatello^a & Vincenzo Busico^a

^a Istituto Chimico dell'Università, Via Mezzocannone, 4-80134, Naples, Italy

Version of record first published: 20 Apr 2011.

To cite this article: Michele Vacatello & Vincenzo Busico (1984): The Structure and Conformation of n-Hydrocarbon Chains in Bilayer Systems in the "Fluid" Phase, *Molecular Crystals and Liquid Crystals*, 107:3-4, 341-357

To link to this article: <http://dx.doi.org/10.1080/00268948408070446>

PLEASE SCROLL DOWN FOR ARTICLE

Full terms and conditions of use: <http://www.tandfonline.com/page/terms-and-conditions>

This article may be used for research, teaching, and private study purposes. Any substantial or systematic reproduction, redistribution, reselling, loan, sub-licensing, systematic supply, or distribution in any form to anyone is expressly forbidden.

The publisher does not give any warranty express or implied or make any representation that the contents will be complete or accurate or up to date. The accuracy of any instructions, formulae, and drug doses should be independently verified with primary sources. The publisher shall not be liable for any loss, actions, claims, proceedings, demand, or costs or damages whatsoever or howsoever caused arising directly or indirectly in connection with or arising out of the use of this material.

The Structure and Conformation of *n*-Hydrocarbon Chains in Bilayer Systems in the “Fluid” Phase

MICHELE VACATELLO and VINCENZO BUSICO

Istituto Chimico dell'Università, Via Mezzocannone, 4-80134 Naples (Italy)

(Received October 3, 1983)

A realistic computer model of a bilayer of hexadecyl groups at a surface area per chain corresponding to that present in systems of biological interest has been obtained using the Monte Carlo technique. Properties evaluated from the model are in good agreement with results of deuterium magnetic resonance (d.m.r.) and X-ray and neutron diffraction experiments, showing that the distribution of matter and the degree of order in the model are not too far from those in real bilayer systems.

The structure of the model bilayer consists of two “single layer” regions, closely related to the plateau of the d.m.r. order parameters, separated by a large interpenetration zone. The conformation of the alkyl chains, though extended along the normal to the layers, is not perturbed to a great extent with respect to the unperturbed model. A uniform filling of the space is obtained in the model in the absence of long range orientational correlations such as the collective tilt postulated in the literature.

INTRODUCTION

We have been investigating the structure and conformation of systems of hydrocarbon molecules in disordered states through the analysis of realistic computer models obtained with the Monte Carlo technique.

A first study¹ dealt with the molecular organization in a long chain *n*-hydrocarbon liquid. The agreement between properties evaluated from the model and both experimental results and theoretical predictions showed that computer models obtained with this technique can be valuable in order to understand the average local situation in

complex systems of this kind. For instance, we were able to show that the strong orientational correlations among adjacent molecules often invoked in the literature are unnecessary to explain the packing of disordered hydrocarbon chains at the correct density and their X-ray diffraction profiles.

More recently, we have modified our method in order to produce a computer model of a monolayer of hexadecyl groups at a surface density corresponding to 0.27 nm^2 per molecule.^{2,3} Very good agreement with experimental results on well characterized systems from our and other laboratories provided confidence in the method and prompted us to extend this investigation to a computer model closer to lipid bilayer systems of biological interest.

The present paper indeed reports on the simulation of a bilayer of hexadecyl groups packed at an average area per chain of 0.32 nm^2 . Simulating a bilayer rather than a monolayer is necessary here in order to reproduce the perturbing effects at the free chain termini due to the interaction of the two counterfacing layers. Such effects, which were shown to be small for the system of ref. 3, are expected to be of some importance in bilayers with a smaller surface density as the one under study.

Preliminary results of the present investigation have been previously published.⁴

THE MODEL

The model system has been obtained with the same procedure and parameters of ref. 3 (0.154 nm bond lengths; tetrahedral valence angles; T , G^+ , G^- torsion angles with $E_g = 2.1 \text{ kJ mol}^{-1}$ and $G^\pm G^\mp$ two bond sequences disallowed; 0.34 nm hard sphere diameter).

A two-dimensionally periodic cell ($a = b = 3.394 \text{ nm}$; $\gamma = 90^\circ$) containing 36 all- G^+ chains with helical axes parallel to the layer normal was initialized with the first chain units in the basal ab plane at the nodes of a hexagonal array. Reflection through a plane at $z = 1.436 \text{ nm}$ gave the initial coordinates of the counterfacing layer, which was shifted parallel to the ab plane in such a way to avoid distances smaller than 0.34 nm between non bonded units in the central part of the bilayer.

Since a methyl group occupies a volume about twice that of a methylene and only one half of a unit in the basal planes belongs to the cell, this gives an average volume per methylene of the order of 0.028 nm^3 .

The system was equilibrated at room temperature with the following mechanisms (for details, see ref. 3):

- a) translations of chains parallel to the *ab* plane
- b) rigid rotations of whole chains around the first units
- c) local changes of torsion angles in the chain interior
- d) changes of torsion angles at the methyl chain ends
- e) overall changes of the molecular conformation in the bilayer environment

subject to the following constraints:

- i) the *z* coordinate of the first unit of each chain was fixed
- ii) distances between non bonded units smaller than 0.34 nm were forbidden
- iii) the basal layers could not be approached at distances smaller than 0.17 nm by chain units other than the first two of each molecule.

We defined a cycle as being made of the following number of attempts to activate the previous mechanisms: 6000 a, 6000 b, 60000 c, 6000 d, 6000 e. Each cycle required about 80 min of CPU on the UNIVAC 1100/80 computer at the University of Naples, giving the following average number of successful moves: 730 a, 410 b, 820 c, 840 d, 520 e. The coordinates of the first unit and the conformation of a selected hexadecyl group at the end of some of the cycles are reported in Table

TABLE I

Coordinates of the first unit (starting from the basal plane) and conformation in the rotational isomeric approximation of one of the hexadecyl groups in the model system at various stages of the calculation

	Cycle <i>n</i>						
	0	2	4	10	14	16	18
<i>x</i>	18.4	16.6	23.2	21.0	18.5	23.3	23.8
<i>y</i>	28.3	32.0	31.2	33.0	29.6	26.3	27.7
1	<i>G</i> ⁺	<i>T</i>	<i>T</i>	<i>T</i>	<i>G</i> ⁻	<i>T</i>	<i>T</i>
2	<i>G</i> ⁺	<i>G</i> ⁺	<i>T</i>	<i>T</i>	<i>T</i>	<i>G</i> ⁺	<i>T</i>
3	<i>G</i> ⁺	<i>T</i>	<i>G</i> ⁻	<i>G</i> ⁺	<i>G</i> ⁻	<i>T</i>	<i>T</i>
4	<i>G</i> ⁺	<i>G</i> ⁻	<i>T</i>	<i>T</i>	<i>T</i>	<i>G</i> ⁻	<i>G</i> ⁺
5	<i>G</i> ⁺	<i>T</i>	<i>G</i> ⁻	<i>G</i> ⁺	<i>G</i> ⁻	<i>T</i>	<i>T</i>
6	<i>G</i> ⁺	<i>T</i>	<i>T</i>	<i>T</i>	<i>T</i>	<i>T</i>	<i>G</i> ⁻
7	<i>G</i> ⁺	<i>G</i> ⁺	<i>T</i>	<i>G</i> ⁻	<i>T</i>	<i>G</i> ⁺	<i>T</i>
8	<i>G</i> ⁺	<i>G</i> ⁺	<i>T</i>	<i>T</i>	<i>T</i>	<i>T</i>	<i>G</i> ⁻
9	<i>G</i> ⁺	<i>T</i>	<i>G</i> ⁺	<i>G</i> ⁻	<i>T</i>	<i>G</i> ⁻	<i>T</i>
10	<i>G</i> ⁺	<i>G</i> ⁺	<i>T</i>	<i>T</i>	<i>T</i>	<i>T</i>	<i>G</i> ⁻
11	<i>G</i> ⁺	<i>T</i>	<i>T</i>	<i>G</i> ⁻	<i>G</i> ⁺	<i>G</i> ⁻	<i>T</i>
12	<i>G</i> ⁺	<i>G</i> ⁻	<i>T</i>	<i>T</i>	<i>T</i>	<i>T</i>	<i>T</i>
13	<i>G</i> ⁺	<i>G</i> ⁻	<i>T</i>	<i>G</i> ⁻	<i>T</i>	<i>T</i>	<i>G</i> ⁺

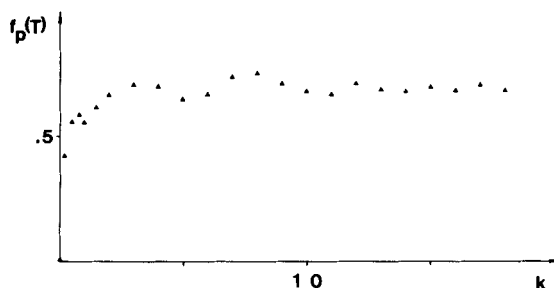


FIGURE 1 The fraction, $f_p(T)$ of bonds in trans conformation as evaluated from the model bilayer at the completion of each cycle or fraction of a cycle versus the cycle number, k .

I, showing that the amount of positional and conformational mobilities provided to the system is sufficiently high to allow a good sampling of the configuration space.

A state of equilibrium, in which all the relevant properties of the model oscillate around an average value, was reached after about 7–11 cycles. Figure 1 shows, as an example, the fraction of bonds in trans conformation as evaluated from the model system at various stages of the equilibration. The results reported in the following are averaged over 50 different system configurations which were stored in memory while performing cycles 15 to 18. We have checked that using cycles 11 to 14 gives practically identical results.

RESULTS AND DISCUSSION

The forces which govern the structure and conformation of systems of long hydrocarbon chains are today fairly well understood. The parameters used in the present calculation to model molecular geometry and torsional potential around the $\text{CH}_2\text{—CH}_2$ bonds are widely accepted and have been shown to reproduce with a high degree of accuracy a large number of experimental results on systems containing polymethylenic sequences.⁵

Using hard spheres to model the continuous interaction energy function $V(r)$ between non bonded methylene units (such as that given in ref. 6; see Figure 2) is more questionable. In the absence of directional interactions, the structure of densely packed liquids is commonly thought to be mainly determined by the repulsive part of the non bonded potential.^{7,8} It has been recently shown⁹ that including the attractive part of $V(r)$ up to a cutoff distance $r_c = 0.50$ nm

does not significantly modify the structure and conformation of a computer model of *n*-hydrocarbon liquids with respect to a similar model for which $r_c = 0.38$ nm. Since the repulsive part of $V(r)$ is a steeply decreasing function of the non bonded distance, the approximation introduced by the use of hard spheres (which leads to a substantial reduction of the computer time needed for the equilibration) can be made relatively small with an appropriate choice of the hard sphere diameter, d_s .

Figure 2 shows that a value of d_s smaller than 0.32 nm would introduce unreasonably short contacts between non bonded methylene units. A value higher than 0.36 nm, on the other hand, would lower the effectiveness of the mechanisms used to sample the configuration space, and would require intramolecular C_i-C_{i+4} non bonded interactions to be handled separately in order not to forbid $G^\pm G^\pm$ two bond sequences. Hence, we take $d_s = 0.34$ nm as a reasonable choice,

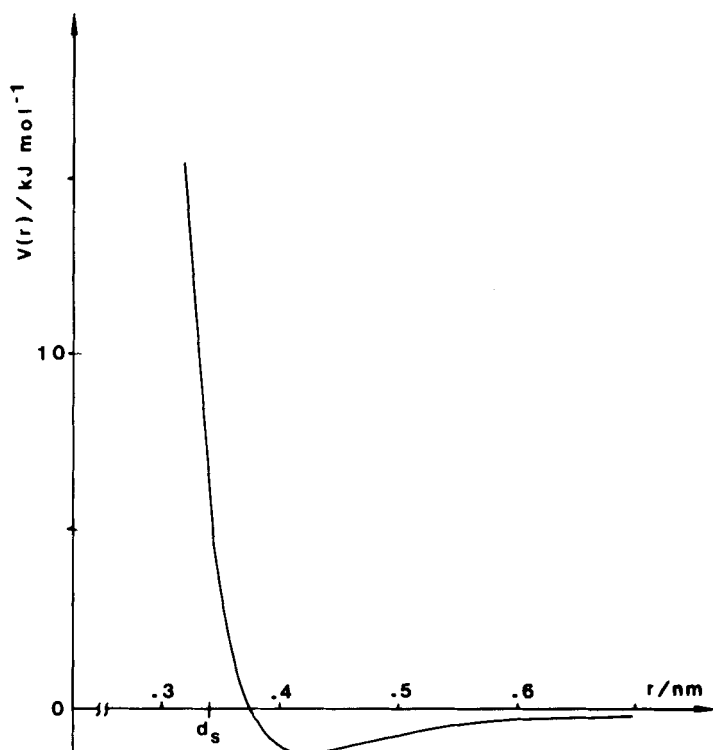


FIGURE 2 The Mason and Kreevoy's non bonded potential function between methylene units.⁶ d_s = the rigid sphere diameter used in this work.

keeping in mind that confidence in the model is to be based on its ability to reproduce known experimental results and to make reasonable predictions of unknowns.

a) Comparison with experiments

Available experimental data giving direct information on the intimate structure of bilayers come essentially from magnetic resonance and neutron diffraction measurements on systems containing selectively deuterated hydrocarbon chains.

Deuterium magnetic resonance (d.m.r.) allows to determine the carbon-deuterium order parameters S_i at the deuterated i th unit (defined as $S_i = \langle 3\langle \cos^2 \theta_i \rangle - 1 \rangle / 2$, θ_i being the angle between a C—D bond vector and the normal to the basal plane). Neutron diffraction gives both the average position of the unit and its extent of positional fluctuation along the layer normal.

Less detailed, but conceptually related information is contained in the X-ray diffraction profiles of bilayers in the “fluid” phase, showing a halo centered around 0.46 nm very similar to that present in the profiles of liquid hydrocarbons.¹⁰

Little is known from the experimental viewpoint about the conformation of the alkyl groups in these systems. There seems to exist, however, a general agreement between various kinds of experiments and theoretical predictions pointing out a fraction of bonds in gauche states not far from 0.3.¹¹

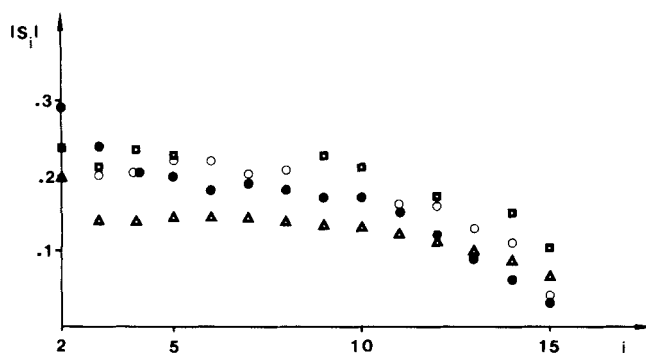


FIGURE 3 Comparison of the absolute value of the C-D order parameters $|S_i|$ (●) evaluated from the model system with values obtained by d.m.r. for the “fluid” phase of a potassium palmitate/water system¹² (Δ), for DPPC¹⁴ (□) and A. Laidlawii membranes¹⁵ (○). The area per alkyl group in planes parallel to the layers corresponds for the experimental systems to 0.35 nm²,¹³ 0.32 nm²,¹⁴ and 0.30 nm²,¹⁵ respectively.

TABLE II

Average distance of various methylene units from the middle of the bilayer as obtained by neutron diffraction on 1,2-dipalmitoyl-*sn*-glycero-3 phosphocholine at 25% (w/w) water and 50 °C¹⁶ and calculated from the model system

unit <i>n</i>	neutron diffraction	this model
4	12.3 ± 1.5	11.3
5	10.5 ± 1.5	10.4
9	8.1 ± 1	6.8
14	3.6 ± 1	3.0
15	1.9 ± 1	2.6

Figure 3 compares the carbon-deuterium order parameters S_i evaluated from our model with values obtained by d.m.r. for the "fluid" phase of a potassium palmitate/water system¹² and for a synthetic¹⁴ and a natural¹⁵ lipid bilayer containing the palmitate chain. The average distance of various methylene units from the bilayer midplane as obtained from the model and from neutron diffraction on 1,2-dipalmitoyl-*sn*-glycero-3 phosphocholine at 25% (w/w) water and 50 °C¹⁶ are compared in Table II. Figure 4 shows the X-ray diffracted intensity calculated as in ref. 1 from the radial distribution function of the model, corrected for its finiteness along

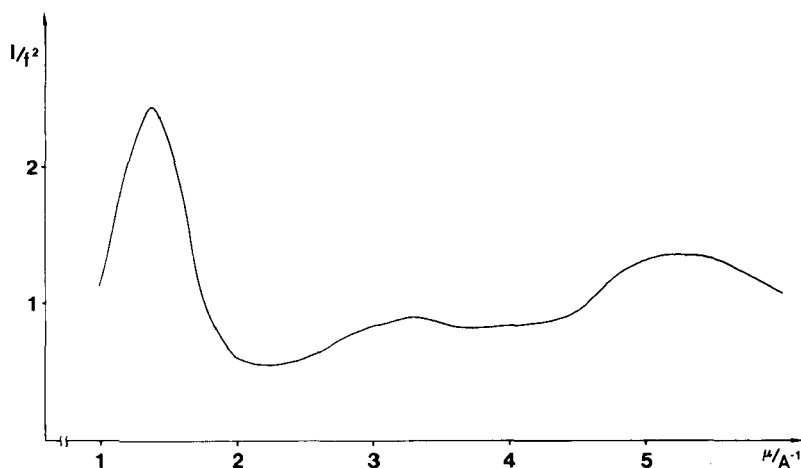


FIGURE 4 The X-ray diffracted intensity calculated from the model as in ref. 1. $I = 4\pi\lambda^{-1}\sin\theta$, where θ is the diffraction angle and λ the X-ray wavelength; f = diffracting power of a methylene unit.

the z axis. The average fraction of bonds in gauche conformations can be seen from the first row of Table IV to be 0.31.

In spite of the great complexity and variety of the experimental systems, the model is seen to provide extremely good results. Apart from the first two methylene units, which are directly influenced by the detailed nature of the polar headgroups, the calculated order parameters show in the correct place the characteristic plateau extending up to units 10–11 which is a common feature of all the investigated lipid bilayers. The average position of the methylene units along the layer normal compares very well with neutron diffraction results, the width of the corresponding distribution curves (see later, Figure 8) being of the same order of that reported in ref. 16. The calculated X-ray diffraction profiles show a broad maximum at 0.46 nm which correctly reproduces both in position and relative intensity the halo present in the profiles of liquid hydrocarbons and lipid bilayers in the “fluid” state. Lastly, the average fraction of bonds in gauche conformations is very close to the expected value.

We want to emphasize that the model presented in this paper does not contain adjustable parameters. Hence, the agreement between calculated and experimental properties proves that all the assumptions and simplifications that constitute the basis of the model are reasonable approximations to the geometry and energetics of a real bilayer, as far as the hydrocarbon region is concerned. This calculation provides then further evidence that, apart from the first few bonds, the detailed nature of the polar heads in lipid bilayers influences the structure and conformation of the alkyl residues mainly because it fixes the area A available per chain in planes parallel to the basal layers. Furthermore, even in a system of hydrocarbon chains with a relatively high degree of orientational correlation, the attractive part of the non bonded potential function seems to play a minor role, all the relevant non bonded interactions being well simulated by a hard sphere potential in which methylene units are given a 0.34 nm diameter.

b) Structure and conformation of the model bilayer

The distribution of orientations of a chain segment comprising three successive methylene units requires, to be adequately described, the specification of at least two independent order parameters. With reference to the local coordinate system of Figure 5, and defining $S_{j'}$ as the order parameter of the j' axis with respect to the layer normal, the carbon-deuterium order parameter S is given with a very good

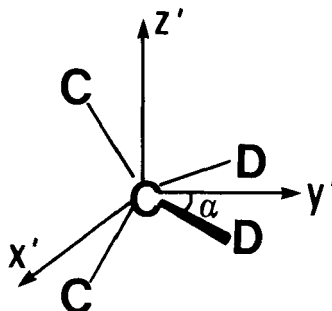


FIGURE 5 The local coordinate system at each CD_2 unit along a deuterated hexadecyl chain.

approximation by $S = S_x \sin^2 \alpha + S_y \cos^2 \alpha$.¹⁷ Since $\cos^2 \alpha$ is very close to $1/3$ and $S_x + S_y + S_z = 0$, it is easily verified that

$$S_z = -2S + (S_x - S_y)/3 \quad (1)$$

S_z is a useful description of the local orientation of the chain backbone, and is often denoted as S_{mol} .¹⁴

Though contrary to expectation, the simplifying hypothesis has often been made in the literature^{18,19} that the motion of a CD_2 group be axially symmetric around its own z' axis. This leads to $S_x = S_y = S$ and $S_z = -2S$.

Table III reports the values of S , $-2S$, S_z , S_x , and S_y as obtained from the model system along the hexadecyl chains. The equality $S_z = -2S$ is seen to be approximately true, while the hypothesis of axial symmetry of the motion around the z' axis is far from being verified. On the other hand, with S_x and S_y of the order of -0.2 and -0.12 , respectively, the error introduced neglecting the last term of Eq. (1) is seen to be of the order of 10% of S_z at most. This conclusion, along with the previous data when opportunely scaled, is completely in line with the results of the thorough analysis of ref. 17.

A much more clarifying picture of the orientational disorder present in the model system is provided by Figure 6, plotting the fraction $f(\theta_z)$ of z' axes oriented at the angle θ_z with respect to the layer normal at units 8 and 15. Curves for units 4 to 10 are remarkably similar to each other, while curves for units 11 to 14 are intermediate between those shown.

The distribution has a pronounced maximum that in all the curves is placed at around $\theta_z = \pi/4$. The decrease of S_z (and the increase of S) beyond unit 10 is explained by a progressive broadening of the

TABLE III

The C-D order parameter and the diagonal elements of the order parameter tensor in the local reference system of Figure 5 (see text) along the hexadecyl groups

unit n	S	$-2S$	$S_{z'}$	$S_{x'}$	$S_{y'}$
2	-0.29	0.58	0.58	-0.30	-0.28
3	-0.23	0.46	0.48	-0.25	-0.23
4	-0.21	0.42	0.40	-0.22	-0.18
5	-0.19	0.38	0.38	-0.22	-0.16
6	-0.18	0.36	0.33	-0.21	-0.12
7	-0.19	0.38	0.35	-0.22	-0.13
8	-0.18	0.36	0.31	-0.21	-0.10
9	-0.17	0.34	0.32	-0.20	-0.12
10	-0.17	0.34	0.32	-0.20	-0.12
11	-0.15	0.30	0.30	-0.17	-0.13
12	-0.12	0.24	0.25	-0.13	-0.12
13	-0.09	0.18	0.19	-0.09	-0.10
14	-0.06	0.12	0.11	-0.05	-0.06
15	-0.03	0.06	0.06	-0.03	-0.03

distribution, with an increasing occurrence of angles close to $\pi/2$, while the position of the maximum is substantially unchanged.

The origin of this effect is easily deduced from the dotted curves plotting the value of $p(\theta_{z'}) = f(\theta_{z'})\sin\theta_{z'}$, which measures the probability for a given chain segment to be found in a unit solid angle at the orientation specified by $\theta_{z'}$; the constant value expected in the isotropic case is shown by the horizontal line in Figure 6.

The principal, obvious effect of the directional constraints present in the model (together with the mutual exclusion of volume among adjacent chains) is to disfavour segment placements at values of $\theta_{z'}$ close to $\pi/2$ or higher. With respect to the isotropic case, this is obtained through an increase of $p(\theta_{z'})$ at small angles, followed by a sharp decrease at around $\theta_{z'} = \pi/4$ which is responsible for the occurrence of the previous peaks in the distribution curves. The overall trend is similar both for units comprised in the plateau region of Figure 3 and for units close to the free ends, with no appreciable shift of the angle corresponding to the drop of $p(\theta_{z'})$. The perturbation with respect to the isotropic case is, however, much higher in the chain interior than at the free ends.

The average value of $\cos\theta_{z'}$ for units comprised in the plateau region turns out to be 0.7, while the increasingly significant proportion of segments oriented at angles close to or higher than $\pi/2$ causes this figure to decrease to about 0.4 at the free methyl ends. The average projection per $\text{CH}_2\text{—CH}_2$ bond along the layer normal is then of the

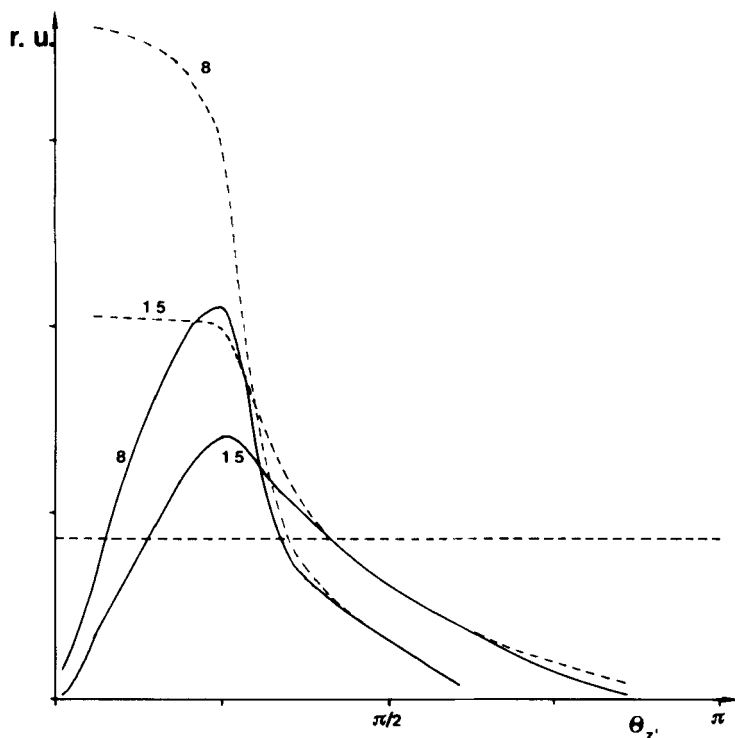


FIGURE 6 The fraction, $f(\theta_{z'})$ of z' axes oriented at the angle $\theta_{z'}$ with respect to the layer normal and $p(\theta_{z'})$ (dotted lines, see text) at units 8 and 15. The horizontal line represents the value of $p(\theta_{z'})$ for an isotropic system. r.u. = relative units.

order of 0.090 nm in the chain interior and decreases smoothly to 0.050 nm for the last bonds. This is seen in Figure 7, which plots the average distance z_i of the chain unit i from the basal layers versus the unit index, i as obtained from the model; data for the monolayer model of ref. 3 are added for comparison.

The average volume per methylene, $v(\text{CH}_2)$ in polymethylenic substances in densely packed disordered states is of the order of 0.028 nm³. This is true for liquid hydrocarbons and polyethylene,²⁰ for all the investigated lipid bilayers in the "fluid" state²¹ and has been confirmed by us even in the high temperature, conformationally disordered solid polymorphs of several series of layer compounds containing long *n*-alkyl groups.⁴

In a layer environment, then, uniform space filling is warranted when the average projection $\Delta \bar{z}$ of the $\text{CH}_2\text{—CH}_2$ bonds along the

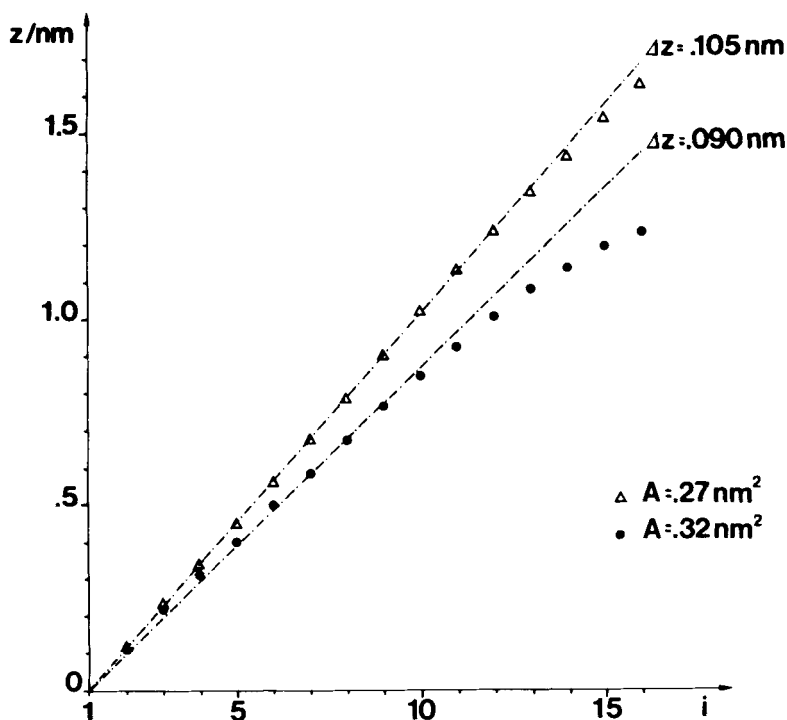


FIGURE 7 The average distance z_i of the chain unit i from the basal layers versus the unit index, i as obtained from the model bilayer. Data for the monolayer of ref. 3 are added for comparison.

layer normal is equal to $v(\text{CH}_2)/A$, A being the area per alkyl group parallel to the layers. This is the case for the model monolayer at $A = 0.27 \text{ nm}^2$, for which the plot of Figure 7 is strictly linear with a slope coincident with $v(\text{CH}_2)/A$, apart from minor deviations at the free methyl ends. Counterfacing monolayers at this surface density are then expected to perturb each other to a relatively little extent.

The same is not true when $A = 0.32 \text{ nm}^2$, the slope varying in this case from about 0.090 nm (coincident with $v(\text{CH}_2)/A$) in the chain interior to smaller values in the middle of the bilayer. Uniform space filling is obtained in the latter region through both an increased proportion of segments directed more or less parallel to the layers or bending back toward the basal planes, and a significant amount of interpenetration between the counterfacing monolayers. This is depicted in Figure 8, showing distribution profiles for units 12, 14 and 16 along the layer normal; the dotted curve represents the fraction of

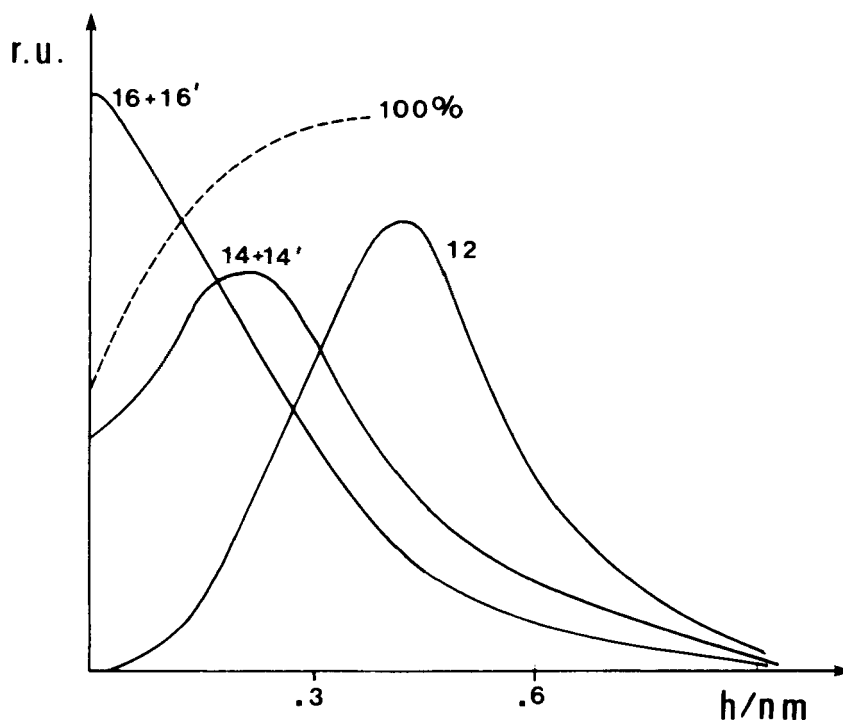


FIGURE 8 Distribution curves (full lines) for units 12, 14 and 16 and fraction of density contributed by each monolayer (dotted lines) versus the distance, h from the middle of the bilayer.

density contributed by each monolayer. The interpenetration zone is seen to be about 0.35 nm wide on both sides, including mainly units from 12 to 16, while the density in the middle of the bilayer receives substantial contributions from units 14 to 16.

The resulting picture of the structure of the model bilayer consists then of two "single layer" regions separated by a central interpenetration zone. The former, mainly including units up to 10–11, are characterized by $\Delta\bar{z} = v(\text{CH}_2)/A$ and closely correspond to the observed plateau of the d.m.r. order parameters; occurrence of chain ends is very infrequent and the space is uniformly filled by placements of segments at angles mainly of the order of $\pi/4$ with respect to the layer normal. The plateau region of bilayers with other values of the surface area per chain could have a similar structure, with the corresponding angle of inclination given by $\cos^{-1}(v(\text{CH}_2)/1.25A)$. Chain terminations are mainly concentrated at the middle of the

bilayer, allowing a larger proportion of segment placements at high angles and a substantial interpenetration of the terminal portion of facing chains.

A quantitative description of the average conformation adopted by the hexadecyl groups in order to realize the previous structure is most interesting because of the conflicting opinions often found in the literature.²² Table IV compares the average fraction, f_p , of sequences in several specified conformations as obtained from the present model with data obtained from the monolayer at $A = 0.27 \text{ nm}^2$ and with the corresponding values calculated for the unperturbed hexadecane molecule ($G^\pm G^\mp$ two bond sequences disallowed) at 300 K, f_u . The perturbing effects provided by the bilayer environment with respect to the unperturbed chain are similar in nature to those described in ref. 3, mainly resulting from an increased tendency to form $(T)_n$ sequences and kinks ($G^\pm TG^\mp$); they are, however, much smaller and the average chain conformation in the bilayer model seems to be not very far from the unperturbed one.

TABLE IV

The average fraction, f_p , of sequences in some specified conformations as obtained from the present model, from the model monolayer of ref. 3 at $A = 0.27 \text{ nm}^2$ and calculated for the unperturbed hexadecane chain ($G^\pm G^\mp$ two bond sequences forbidden) at 300 K, f_u

sequence	f_p		f_u
	$A = 0.27 \text{ nm}^2$	$A = 0.32 \text{ nm}^2$	
T	0.79	0.69	0.64
TT	0.60	0.45	0.38
TG^\pm	0.098	0.12	0.13
$G^\pm G^\pm$	0.013	0.034	0.047
TTT	0.52	0.32	0.22
$G^\pm TG^\pm$	0.014	0.021	0.028
$G^\mp TG^\pm$	0.033	0.031	0.028
$TG^\pm T$	0.085	0.097	0.097
$TTTT$	0.44	0.23	0.13
$TG^\pm TG^\mp$	0.031	0.026	0.020
$G^\pm TG^\mp T$	0.031	0.026	0.020
$TG^\pm TG^\pm$	0.014	0.019	0.020
$G^\pm TG^\pm T$	0.012	0.016	0.020
$TTTTT$	0.39	0.17	0.078
$G^\pm TG^\mp TT$	0.020	0.016	0.012
$G^\pm TG^\pm TT$	0.005	0.007	0.012
$G^\pm TG^\mp TG^\pm$	0.006	0.005	0.004
$G^\pm TTTG^\mp$	0.008	0.011	0.010
$G^\pm TTTG^\pm$	0.004	0.007	0.010
$TG^\pm G^\pm TT$	0.002	0.007	0.015

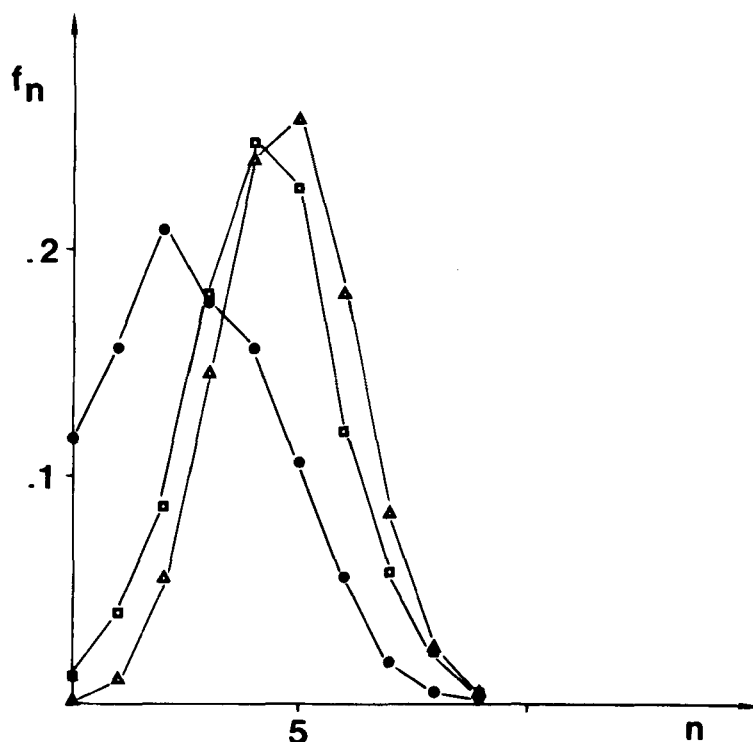


FIGURE 9 The fraction, f_n , of chains in the model system having n bonds in gauche conformations versus n . Δ , unperturbed chain; \square , this model; \bullet , monolayer of ref. 3.

This is confirmed by inspection of Figure 9, showing the fraction of chains having a given number of bonds in gauche conformations: the distribution at the larger value of the surface area is seen to be very similar to that found for the unperturbed chain, while a decrease of A to 0.27 nm^2 implies a substantial shift toward conformations with a reduced number of gauche bonds.

Interestingly, the local chain conformation is found quite uniform in the plateau region and different from that present in the interpenetration zone. For instance, TTT and G^+TG^+ sequences represent about 36% and 1.7%, respectively, of all three bond sequences in the plateau region, while the corresponding values in the interpenetration zone are almost coincident with the unperturbed ones (0.22 and 0.028). The strong odd-even effects found by us and in ref. 23 for systems at a higher surface density are less pronounced or even absent in the present model, depending on the particular conformational sequence considered.

We have investigated the possible presence of local orientational cooperativity (beyond that imposed by the common orientation along the z axis) by evaluating $\langle \cos \psi(z, r) \rangle$ and $\langle \cos^2 \psi(z, r) \rangle$, $\psi(z, r)$ being the angle between the projections on the ab plane of $C_{i-1} - C_{i+1}$ and $C_{k-1} - C_{k+1}$ vectors with units C_i and C_k (belonging to different chains) at distance r and comprised in a layer 0.1 nm thick at a height z with respect to the basal plane. Such parameters are expected to average to 0 and 0.5, respectively, in the absence of orientational cooperativity. They are found to be slightly higher than these values only for touching segments, quite irrespective of z . We conclude then that strong local orientational correlations, such as collective tilts of the chains with respect to the layer normal, are not peculiar features of the bilayer arrangement.

CONCLUSIONS

This paper presents a realistic computer model of a bilayer of n -hexadecyl groups at a surface density similar to that found in systems of biological interest. Experimental results from d.m.r. and neutron scattering, as well as the X-ray diffraction profiles, are correctly reproduced, showing that the distribution of matter and the relative orientation of chain segments in the model are not too far from those in real systems.

The model is characterized by the presence of two "single layer" regions separated by a large interpenetration zone. The plateau in the d.m.r. order parameters seems to be closely associated with the former, in which the average orientation and conformation of the chain segments do not depend to a great extent on the distance from the basal layers.

The interpenetration zone is about 0.7 nm wide, mainly includes the last five chain units on each side and is associated with a massive occurrence of chain terminations, resulting in an increase of the area available per chain. Uniform space filling is reached here through placements of segments at angles θ_z , close to $\pi/2$ and interpenetration of facing chain ends.

Our conclusions are in good qualitative agreement with those derived from the lattice model of Dill and Flory (ref. 8), in which chain ends and an increase of lateral placements are suggested to be responsible for the drop in the order parameters at the middle of a bilayer. Moreover, increasing the surface density is predicted in ref. 8 to result in higher order parameters and segregation of chain ends at higher

values of z ; this is confirmed by comparison of the results of the present calculation with those obtained by us in ref. 3.

The conformation of the alkyl groups in the plateau region is characterized by an increased tendency toward the formation of all trans sequences and kinks, with respect to the unperturbed model. With reference to the monolayer at $A = 0.27 \text{ nm}^2$, however, this tendency is much smaller for the present model. Hence, the denomination of "perturbed random coil" proposed by Gruen¹¹ to identify the conformational state of the alkyl groups in bilayer membranes appears fully adequate. The role of kinks appears to have been overemphasized in the past, though it may become important for systems with a higher surface density.

Acknowledgments

We thank Prof. Paolo Corradini for his interest in this work and for many helpful discussions. Financial help from the C.N.R. (Consiglio Nazionale delle Ricerche) and from the Ministry of Public Education of Italy is gratefully acknowledged.

References

1. M. Vacatello, G. Avitabile, P. Corradini and A. Tuzi, *J. Chem. Phys.*, **73**, 548 (1980).
2. M. Vacatello, V. Busico and P. Corradini, *J. Chem. Phys.*, **78**, 590 (1983).
3. M. Vacatello, V. Busico and P. Corradini, *Gazz. Chim. Ital.*, in press.
4. V. Busico and M. Vacatello, *Mol. Cryst. Liq. Cryst.*, **97**, 195 (1983).
5. P. J. Flory, "Statistical Mechanics of Chain Molecules," Wiley, Interscience, New York, N.Y., 1969.
6. E. A. Mason and M. M. Kreevoy, *J. Am. Chem. Soc.*, **77**, 5808 (1955).
7. P. J. Flory and G. Ronca, *Mol. Cryst. Liq. Cryst.*, **54**, 289 (1979).
8. K. A. Dill and P. J. Flory, *Proc. Natl. Acad. Sci. U.S.A.*, **77**, 3115 (1980).
9. G. Avitabile and A. Tuzi, *J. Polym. Sci., Polymer Phys. Ed.*, **21**, 2379 (1983).
10. D. Chapman, R. M. Williams and B. D. Ladbroke, *Chem. Phys. Lipids*, **1**, 445 (1967).
11. D. W. R. Gruen, *Chem. Phys. Lipids*, **30**, 105 (1982).
12. J. H. Davis and K. R. Jeffrey, *Chem. Phys. Lipids*, **20**, 87 (1977).
13. B. Mely, J. Charvolin and P. Keller, *Chem. Phys. Lipids*, **15**, 161 (1975).
14. A. Seelig and J. Seelig, *Biochemistry*, **13**, 4839 (1974).
15. G. W. Stockton, K. G. Johnson, K. W. Butler, A. P. Tulloch, Y. Boulanger, I. C. P. Smith, J. H. Davis and M. Bloom, *Nature (London)*, **269**, 267 (1977).
16. G. Zaccari, G. Büldt, A. Seelig and J. Seelig, *J. Mol. Biol.*, **134**, 693 (1979).
17. J. P. Meraldi, *Chem. Phys. Lipids*, **28**, 227 (1981).
18. J. Seelig, *Quarterly Rev. Biophys.*, **10**, 353 (1977).
19. E. Oldfield, M. Meadows, D. Rice and R. Jacobs, *Biochemistry*, **17**, 2727 (1978).
20. W. Dollhopf, H. P. Grossman and U. Leute, *Coll. Polym. Sci.*, **259**, 267 (1981).
21. B. P. Gaber and W. L. Peticolas, *Biochim. Biophys. Acta*, **465**, 260 (1977).
22. P. J. Quinn and D. Chapman, *Critical Rev. Biochem.*, **8**, 1 (1980).
23. P. Van der Ploeg and H. J. C. Berendsen, *J. Chem. Phys.*, **76**, 3271 (1982).